Dequantization of a signal from two parallel quantized observations

Vojtěch Kovanda
Dept. of telecommunications
Brno University of Technology
Czech Republic
xkovan07@vutbr.cz

Pavel Rajmic
Dept. of telecommunications
Brno University of Technology
Czech Republic
pavel.rajmic@vut.cz

***Abstract*—We propose a technique of signal acquisition using a combination of two devices with different sampling rates and quantization accuracies. Subsequent processing involving sparsity regularization enables us to reconstruct the signal at such a sampling frequency and with such a bit depth that was not possible using the two devices independently. Objective and subjective tests show the superiority of the proposed method in comparison with alternatives.**

***Index Terms*—Dequantization, bit depth, multichannel, audio, optimization, sparsity, analog-to-digital conversion.**

I. Introduction

In the analog to digital (A/D) conversion, two qualities play a crucial role. The sampling frequency determines how broad the signal spectrum is that can be acquired, while the number of bits used for representing signal samples governs their accuracy [1]. In any particular application, a combination of the sampling frequency and the quantization step that is adequate is required. For demanding applications, however, a proper combination of the parameters can imply a high price of the A/D conversion unit.

In this paper, we propose a system that overcomes the described property via employing two parallel signal acquisition branches. One branch consists of an A/D converter with a high sampling frequency but a coarse quantization. The second branch involves a significantly more accurate quantizer; nevertheless, it operates at a low sampling frequency. The scheme of the system is in Fig. 1. The goal is to reconstruct a signal as close as possible to the original signal, provided the two different observations $\mathbf{y}_1, \mathbf{y}_2$.

If the proposed concept proves beneficial, it could allow employing cheaper components to provide an acquisition quality comparable to high-end devices. The approach could even make some kind of measurements accessible — remember, for instance, the one-pixel camera [2] in image processing, which represents a silly concept at first sight, but it is practically motivated by the high price of infrared sensors. Naturally, the estimation of the original signal from $\mathbf{y}_1, \mathbf{y}_2$ is not straightforward and comes at the cost of computation.

Related work. Increasing the sampling frequency and the quantization resolution of an A/D converter has always been of the interest to the signal processing community. The parallel scheme in Fig. 1 does not represent an entirely new idea: As regards the sampling speed, the physical limit of a sampling device can be bypassed via involving multiple A/D converters that are time-interleaved. Such an idea is actually a special case of the so-called multirate filterbank A/D conversion concept [3], [4]. To increase the resolution in value within the A/D conversion, a similar trick of an array of quantizers with different offsets in value can be applied [5].

In the mentioned approaches, no property of the analog signal is utilized, except its bandwidth. Additional signal characteristics can yet be exploited for the increase of sampling frequency or resolution, as a postprocessing step. This has been demonstrated in various signal processing fields, such as image superresolution [6], audio dequantization [7] or compressive sampling [8], [9]. An approach to increasing the sampling frequency of the A/D conversion has been presented in [10]. The authors showed that when the observed signal from a low-frequency A/D converter is understood as the subsampled version of a desired signal sampled at a high-frequency, it can be estimated via optimization involving the signal sparsity assumption in a proper representation system.

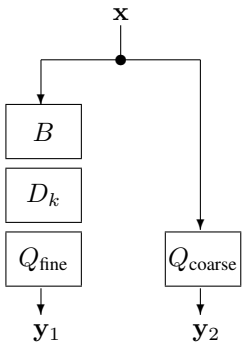

Fig. 1. Scheme of the parallel conversion. In one branch, the original signal $\mathbf{x}$ goes through an anti-aliasing filter B, then the subsampling operator D_k, and finally the quantization with a high-resolution Q_{fine}, producing the observation $\mathbf{y}_1$. The second branch does not alter the sampling frequency and only quantizes the signal with a low-resolution Q_{coarse}. Note that in practice, $\mathbf{x}$ would come in as an analog signal; in our treatment, $\mathbf{x}$ already is assumed in the discrete time.

The work was supported by the Czech Science Foundation (GAČR) Project No. 23-07294S.

A side effect of increasing the effective bit depth is even demonstrated, due to inherent oversampling. Dequantization of audio using different prior assumptions has also been studied [7], [11], [12], [13], [14]. However, these methods only rely on a single channel, which is in contrast to our approach, which combines two parallel sources of quantized audio information to achieve dequantization. We are not aware of any other multichannel dequantization method.

II. Method

The proposed means of signal acquisition is depicted in Fig. 1. The parameters affecting the observations $\mathbf{y}_1, \mathbf{y}_2$ are:

- the sampling frequency of the right-hand branch
- the sampling frequency of the left branch, k-times lower due to the presence of D_k,
- the bit depths of the quantizers Q_{fine} and Q_{coarse},
- the properties of the low-pass filter B.

Due to the involvement of lossy components in the acquisition, the estimation of $\mathbf{x}$ back from $\mathbf{y}_1, \mathbf{y}_2$ is clearly an ill-posed problem. As such, a kind of regularization has to be introduced. As one of the options, we will in this paper make use of the sparsity of an audio signal in the time-frequency domain. Therefore, our recovery task can be written as

$$\hat{\mathbf{x}} = \underset{\mathbf{x}\in\mathbb{R}^L}{\arg\min} \quad \lambda\|A\mathbf{x}\|_1 + \imath_{\Gamma_{\text{fine}}}(D_k B\mathbf{x}) + \imath_{\Gamma_{\text{coarse}}}(\mathbf{x}). \qquad (1)$$

The operator A transforms an audio signal from $\mathbb{R}^L$ to the time-frequency domain $\mathbb{C}^P$ [15], and the sparsity of such a representation is quantified by the convex ℓ_1-norm $\|\cdot\|_1$ [16]. The functions $\imath_{\Gamma_{\text{fine}}}$ and $\imath_{\Gamma_{\text{coarse}}}$ are the indicator functions [17] enforcing the estimate to lie within the quantization levels corresponding to the operators Q_{fine} and Q_{coarse}, respectively. The indicator functions thus secure consistency of the solution with the observations, while the sparsity-related term promotes natural audio signals. Finally, the scalar $\lambda > 0$ is a weight which in theory could be omitted but can be used to influence the convergence of the numerical algorithm.

The problem (1) is convex and can be solved, for instance, by the Condat–Vũ algorithm (CVA) [18], [19], which utilizes proximal operators [17] corresponding to the functions involved in (1). The CVA for our problem is in Alg. 1. The asterisk denotes the adjoint of a linear operator; the adjoint of B is simply a filtering with the impulse response flipped in time. The operator $\text{clip}_\lambda(\cdot)$ clips the input vector elementwise such that the output samples reside in the interval $[-\lambda, \lambda]$.

As for the scalars τ, σ, the convergence of CVA is guaranteed if it holds $\tau\sigma\|A^*A + (D_kB)^*(D_kB) + Id^*Id\| \leq 1$. Using the properties of operator norms, we can arrive at a weaker (still sufficient) condition $\tau\sigma(2 + \|\mathbf{b}\|_1^2) \leq 1$, where $\|\mathbf{b}\|_1$ is the ℓ_1-norm of the impulse response corresponding to B. Also, we have utilized the assumption that A corresponds to a tight Parseval frame, which is achieved via a suitable selection of transfrom parameters [20]. The parameter ρ has to satisfy $\rho \in]0, 2[$.

Algorithm 1: Condat–Vũ algorithm (CVA) solving (1)

Choose parameters $\tau, \sigma, \rho > 0$ and initial values $\mathbf{x}^{(0)} \in \mathbb{R}^L,\ \mathbf{u}_1^{(0)} \in \mathbb{C}^P, \mathbf{u}_2^{(0)} \in \mathbb{R}^{L/k}, \mathbf{u}_3^{(0)} \in \mathbb{R}^L$.

for $i = 0, 1, \ldots$ **do**

$$\tilde{\mathbf{x}}^{(i+1)} = \mathbf{x}^{(i)} - \tau(A^*\mathbf{u}_1^{(i)} - B^*D_k^*\mathbf{u}_2^{(i)} - \mathbf{u}_3^{(i)})$$
$$\mathbf{x}^{(i+1)} = \rho\tilde{\mathbf{x}}^{(i+1)} + (1-\rho)\mathbf{x}^{(i)}$$
$$\tilde{\mathbf{u}}_1^{(i+1)} = \text{clip}_\lambda(\mathbf{u}_1^{(i)} + \sigma A(2\tilde{\mathbf{x}}^{(i+1)} - \mathbf{x}^{(i)}))$$
$$\mathbf{u}_1^{(i+1)} = \rho\tilde{\mathbf{u}}_1^{(i+1)} + (1-\rho)\mathbf{u}_1^{(i)}$$
$$\mathbf{p}_2 = \mathbf{u}_2^{(i)} + \sigma D_k B(2\tilde{\mathbf{x}}^{(i+1)} - \mathbf{x}^{(i)}) \ \text{\% auxiliary}$$
$$\tilde{\mathbf{u}}_2^{(i+1)} = \mathbf{p}_2 - \sigma\,\text{proj}_{\Gamma_{\text{fine}}}(\mathbf{p}_2/\sigma)$$
$$\mathbf{u}_2^{(i+1)} = \rho\tilde{\mathbf{u}}_2^{(i+1)} + (1-\rho)\mathbf{u}_2^{(i)}$$
$$\mathbf{p}_3 = \mathbf{u}_3^{(i)} + \sigma(2\tilde{\mathbf{x}}^{(i+1)} - \mathbf{x}^{(i)}) \ \text{\% auxiliary}$$
$$\tilde{\mathbf{u}}_3^{(i+1)} = \mathbf{p}_3 - \sigma\,\text{proj}_{\Gamma_{\text{coarse}}}(\mathbf{p}_3/\sigma)$$
$$\mathbf{u}_3^{(i+1)} = \rho\tilde{\mathbf{u}}_3^{(i+1)} + (1-\rho)\mathbf{u}_3^{(i)}$$

end

III. Experiment

For the numerical experiment, we selected recordings of solo instruments. Such signals exhibit a great time-frequency sparsity, which the proposed reconstruction is regularized with. Five of the audio excerpts are our own recordings, and other three are picked from the EBU database[1]. All audio is sampled at 48 kHz, in the 24-bit resolution (further on, we use the abbreviation bps for bits per sample). The excerpts are 6 seconds long. Audio has been peak-normalized to make the most of the available dynamic range.

Regarding the acquisition channels (see Fig. 1), Q_{coarse} operates at the bit depth varying between 4 and 16 bps, while the bit depth of Q_{fine} ranges between 10 and 24 bps. The quantization is uniform (linear PCM), as is typical in audio [1]. We use the mid-riser distribution of quantization levels, in line with [7]. In all experiments, the downsampling factor $k = 4$ is fixed, as is the low pass filter B, which has been designed by the Matlab Filter Designer as a FIR filter using the equiripple method. For the purpose of the reconstruction, however, the properties of B are not crucial; actually, the proposed system would be applicable even if the filter would not be present.

A. Objective evaluation

We measure the performance of the algorithms using objective metrics: the common signal-to-distortion ratio (SDR) and the objective difference grade (ODG) provided by the PEMO-Q computational psychoacoustic model [21]. The ODG scale ranges from -4 to 0 (worst to best). We are interested in the scores of our estimate $\hat{\mathbf{x}}$, compared with the known reference signal $\mathbf{x}$. We also compare against the reconstruction achievable from the right-hand channel only, i.e., from the result of the Chambolle–Pock algorithm (CPA) applied to the observation $\mathbf{y}_2$; the CPA was taken from [7].

The results are condensely presented in Figs. 2 and 3. Instructions how to read the graphs are in the captions. As

[1] https://qc.ebu.io/testmaterial/522/

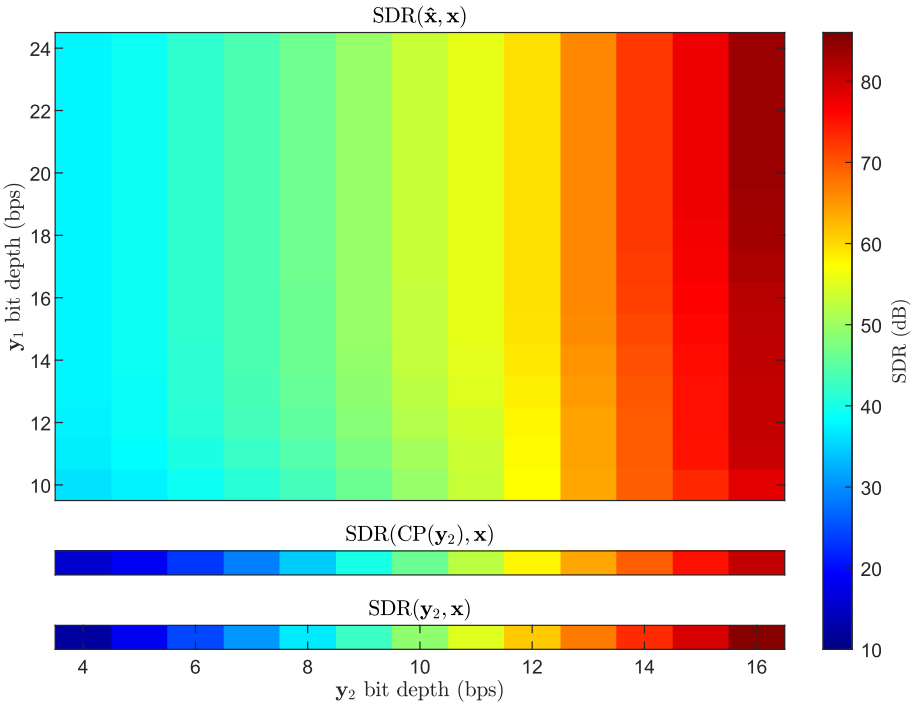

Fig. 2. Dequantization results in terms of the SDR; averages across test signals are presented. Each field in the main grid corresponds to a combination of bit depths. The colors code the SDR value of our reconstruction $\hat{\mathbf{x}}$ related to the original signal $\mathbf{x}$ (a warmer color indcates a closer estimate). The horizontal strip just below the main grid shows the SDR of the one-branch reconstruction, $\mathrm{CP}(\mathbf{y}_2)$. The bottom strip presents the SDR of $\mathbf{y}_2$ without postprocessing.

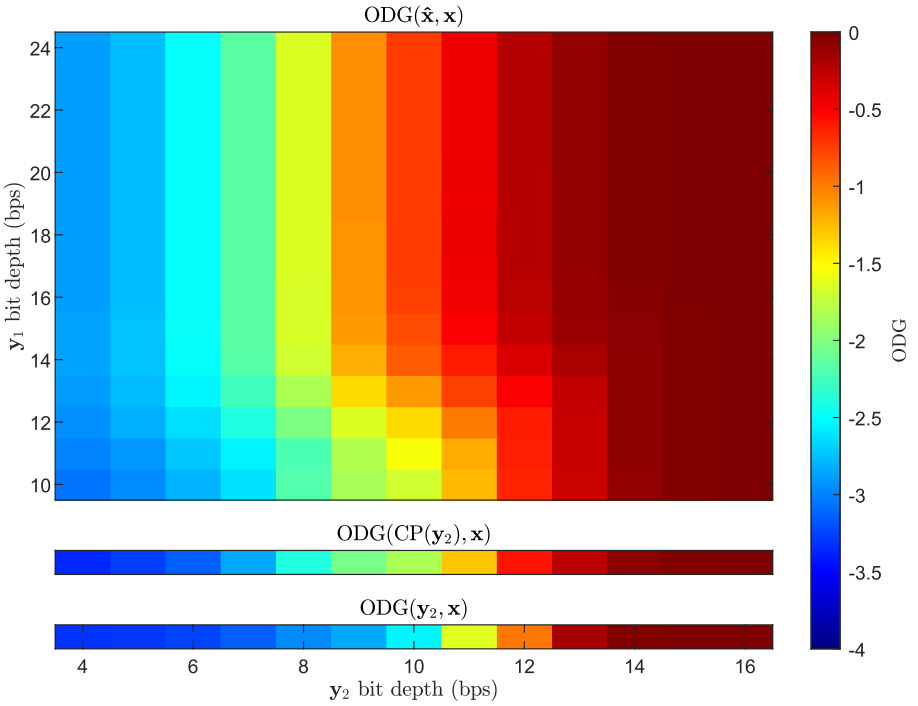

Fig. 3. Dequantization results in terms of the ODG, presented in analogy with Fig. 2.

an example, take the case of 10 bps of the $\mathbf{y}_2$ branch. From the graph, we can see that the 10-bit $\mathbf{y}_2$ without processing provides an average SDR of 48.01 dB. Application of the CPA to $\mathbf{y}_2$ decreases the SNR to 46.40 dB. Involving the $\mathbf{y}_1$ of 20 bps into the reconstruction provides a SDR of 53.11 dB. The same combination of bit depths but now in terms of the ODG scale, we see that the CPA increases the ODG of $\mathbf{y}_2$ from −2.54 to −1.84. Any number of additional bits in the $\mathbf{y}_1$ branch further increases the fidelity; for instance the 20-bps case yields ODG of −0.74.

It was expected that for complex sounds, a lower quality of reconstruction will be exhibited than in the case of the solo instruments. However, the reconstruction results of a mixture of four recordings (two violin, cello, piano) were comparable to the solo-instrument cases as presented in the figures.

B. Subjective evaluation

In addition to the objective metrics, a formal listening test has been performed on the audio excerpts. The combination of 16 and 8 bits for $\mathbf{y}_2$ and $\mathbf{y}_1$ respectively was selected. In particular, the 8-bit depth was chosen because a dithered version of $\mathbf{y}_2$ could be involved in the evaluation this way. Dithering is a technique of transforming the unpleasant quantization noise into a more statistically stable noise, making the result more pleasant to listen to [1]. In our case, Izotope's MBIT+ dithering algorithm[2] has been applied when converting $\mathbf{x}$ to the 8-bit resolution.

The participants have undergone a MUSHRA-type test [22]. Each test signal was presented in their five forms: in the original $\mathbf{x}$, in the dithered form of $\mathbf{x}$, as $\mathbf{y}_2$, as $\mathrm{CP}(\mathbf{y}_2)$ and as $\hat{\mathbf{x}}$. The participants were asked to score the quality of the signals. The test was run in a quiet music studio, using a professional sound card and headphones. The listening conditions were identical for all the 18 participants.

The results are summarized in Fig. 4 in the form of a boxplot. We can see that the proposed method ($\hat{\mathbf{x}}$) was evaluated very good. Actually, it has often been assigned a score better than the score of the original signal (this fact is not apparent from the plot). The described observation is probably due to the fact that noticeable amount of noise was present in some of the original signals. The proposed optimization problem (1) in principle represents a constrained denoising task, thus some participants liked the denoised $\hat{\mathbf{x}}$ more than $\mathbf{x}$. Boxplots of the dithered signal and the CPA show almost identical means and medians, but the CPA exhibits a larger variance. The unprocessed $\mathbf{y}_2$ was evaluated the worse as expected.

C. Computational considerations

Algorithm 1 was run for 200 iterations. Regarding the plots of the SDR, the maximum SDR achieved within these 200 iterations has been presented. In particular cases, a small additional SDR improvement can be gained by running more than 200 iterations; nevertheless, increasing the iteration count does not bring an improvement in most cases; typically, it is

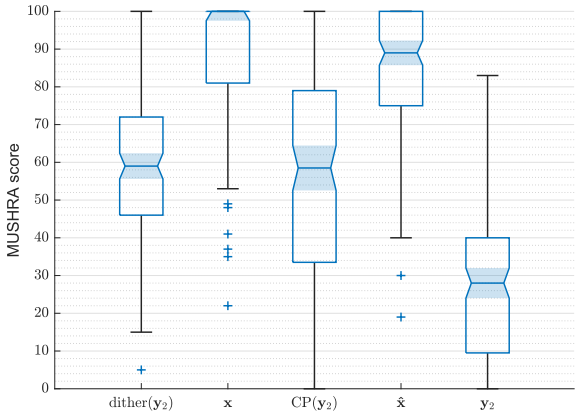

Fig. 4. A boxplot showing the distribution of scores in the listening test.

the other way round. Such an interesting effect is due to the presence of the ℓ_1 norm in (1): After reaching a good SDR within the constraints given by Γ_{fine} and Γ_{coarse}, the ℓ_1 norm starts to prevail, and as a lower $\|A\mathbf{x}\|_1$ is promoted, the signal is pushed towards lower quantization decision levels, therefore worsening the SDR [7]. The same effect is observable in the strip corresponding to the CPA in Fig. 2, since the CPA utilizes the ℓ_1 norm as well. The described effect is nevertheless not present in the ODG scores, and no significant improvement typically occurred with a greater number of iterations. Thus, the ODG value was taken from the iteration no. 200.

Note that in Alg. 1, the parameter λ appears solely in connection with the clip operator. For each particular combination of the bit depths of the quantizers, a different choice of λ is advantageous as it speeds up the convergence and yields better results. Finding a right λ requires hand-on tuning, but we took advantage of published values in [7] as the starting point.

A single iteration of the CVA takes about 0.18 seconds on a laptop with Intel 1.7 GHz CPU and 16 GB RAM. Thus, a 6-seconds-long signal is reconstructed in about 36 seconds.

IV. Conclusion

We have shown the possibility of reconstructing the desired signal from two parallel acquisition branches. Our algorithm scored well in both objective and subjective tests. In future, testing at higher sampling rates is necessary.

Further extensions come naturally. For example, our approach exploits the simplest form of sparsity available; one could think about employing advanced signal priors such as the social sparsity [23] or the phase-consistency [24]. In such cases, only parts of the CVA algorithm would change. Generalization to nonuniform quantization would be straightforward. We have demonstrated the concept in field of audio; however, the concept is general enough to be translated to image or video processing fields, with suitable regularizers. Finally, the concept allows increasing the sampling frequency beyond the one physically available in a device [10], i.e., superresolution.

Codes for Matlab are publicly available.[3]

[2]https://downloads.izotope.com/docs/rx6/39-dither/index.html

[3]https://github.com/rajmic/parallel-dequantization

REFERENCES

[1] J. Watkinson, *The Art of Digital Audio*, Focal Press, 2001.

[2] M.F. Duarte, M.A. Davenport, D. Takhar, J.N. Laska, Ting Sun, K.F. Kelly, and R.G. Baraniuk, "Single-pixel imaging via compressive sampling," *IEEE Signal Processing Magazine*, vol. 25, no. 2, pp. 83–91, 2008.

[3] A. Petraglia and M.A.A. Pinheiro, "Effects of quantization noise in parallel arrays of analog-to-digital converters," in *Proceedings of IEEE International Symposium on Circuits and Systems – ISCAS '94*, 1994, vol. 5, pp. 337–340.

[4] P. Lowenborg and H. Johansson, "Quantization noise in filter bank analog-to-digital converters," in *The 2001 IEEE International Symposium on Circuits and Systems (ISCAS)*, 2001, vol. 2, pp. 601–604.

[5] Jian Gao, Peng Ye, Hao Zeng, Zhixiang Pan, Yu Zhao, Hao Li, and Jie Meng, "Theory of quantization-interleaving adc and its application in high-resolution oscilloscope," *IEEE Access*, vol. 7, pp. 156722–156732, 2019.

[6] Filip Šroubek, Jan Flusser, and Gabriel Cristóbal, "Super-resolution and blind deconvolution for rational factors with an application to color images," *The Computer Journal*, vol. 52, no. 1, pp. 142–152, 2009.

[7] Pavel Záviška, Pavel Rajmic, and Ondřej Mokrý, "Audio dequantization using (co)sparse (non)convex methods," in *2021 IEEE International Conference on Acoustics, Speech and Signal Processing (ICASSP)*, Toronto, Canada, 2021, pp. 701–705.

[8] Emmanuel J. Candes and Michael B. Wakin, "An introduction to compressive sampling," *IEEE Signal Processing Magazine*, vol. 25, no. 2, pp. 21–30, 2008.

[9] Marie Mangová, *Increasing Resolution in Perfusion Magnetic Resonance Imaging Using Compressed Sensing*, Ph.d. thesis, Brno University of Technology, 2018.

[10] Aldo Baccigalupi, Mauro D'Arco, Annalisa Liccardo, and Rosario Schiano Lo Moriello, "Compressive sampling-based strategy for enhancing ADCs resolution," *Measurement*, vol. 56, pp. 95–103, 2014.

[11] C. Brauer, Z. Zhao, D. Lorenz, and T. Fingscheidt, "Learning to dequantize speech signals by primal-dual networks: an approach for acoustic sensor networks," in *2019 IEEE International Conference on Acoustics, Speech and Signal Processing (ICASSP)*, May 2019, pp. 7000–7004.

[12] Lucas Rencker, Francis Bach, Wenwu Wang, and Mark D. Plumbley, "Sparse recovery and dictionary learning from nonlinear compressive measurements," *IEEE Transactions on Signal Processing*, vol. 67, no. 21, pp. 5659–5670, Nov. 2019.

[13] P. T. Troughton, "Bayesian restoration of quantised audio signals using a sinusoidal model with autoregressive residuals," in *Proceedings of the 1999 IEEE Workshop on Applications of Signal Processing to Audio and Acoustics. WASPAA'99 (Cat. No.99TH8452)*, Oct. 1999, pp. 159–162.

[14] Hyun-Wook Yoon, Sang-Hoon Lee, Hyeong-Rae Noh, and Seong-Whan Lee, "Audio dequantization for high fidelity audio generation in flow-based neural vocoder," in *Proc. Interspeech 2020*, Shanghai, China, Oct. 2020, pp. 3545–3549.

[15] Karlheinz Gröchenig, *Foundations of time-frequency analysis*, Birkhäuser, 2001.

[16] David L. Donoho and Michael Elad, "Optimally sparse representation in general (nonorthogonal) dictionaries via ℓ_1 minimization," *Proceedings of The National Academy of Sciences*, vol. 100, no. 5, pp. 2197–2202, 2003.

[17] P.L. Combettes and J.C. Pesquet, "Proximal splitting methods in signal processing," *Fixed-Point Algorithms for Inverse Problems in Science and Engineering*, vol. 49, pp. 185–212, 2011.

[18] Laurent Condat, "A generic proximal algorithm for convex optimization—application to total variation minimization," *Signal Processing Letters, IEEE*, vol. 21, no. 8, pp. 985–989, Aug. 2014.

[19] B. C. Vũ, "A splitting algorithm for dual monotone inclusions involving cocoercive operators," *Advances in Computational Mathematics*, vol. 38, no. 3, pp. 667–681, Apr. 2013.

[20] O. Christensen, *An Introduction to Frames nad Riesz Bases*, Birkhäuser, Boston-Basel-Berlin, 2003.

[21] R. Huber and B. Kollmeier, "PEMO-Q—A new method for objective audio quality assessment using a model of auditory perception," *IEEE Trans. Audio Speech Language Proc.*, vol. 14, no. 6, pp. 1902–1911, Nov. 2006.

[22] "Recommendation ITU-R BS.1534-3: Method for the subjective assessment of intermediate quality level of audio systems," 2015.

[23] M. Kowalski, K. Siedenburg, and M. Dörfler, "Social sparsity! neighborhood systems enrich structured shrinkage operators," *Signal Processing, IEEE Transactions on*, vol. 61, no. 10, pp. 2498–2511, 2013.

[24] Tomoro Tanaka, Kohei Yatabe, and Yasuhiro Oikawa, "Phase-aware audio inpainting based on instantaneous frequency," in *2021 Asia-Pacific Signal and Information Processing Association Annual Summit and Conference (APSIPA ASC)*, 2021, pp. 254–258.